Directional coupler based on metal-insulator-metal plasmonic waveguide

MANOJ MISHRA[1], VISHAKHA TAKHAR[1,2], SOUMENDU JANA[3,*]
[1]*Department of Physics, Mody University of Science and Technology, SLAS, Lakshmangarh-332311, Sikar, Rajasthan, India*
[2]*Department of Physics, Indian Institute of Technology Gandhinagar, Palaj, Gandhinagar- 382355, Gujarat, India*
[3]*School of Physics and Materials Science, Thapar Institute of Engineering & Technology, Patiala-147004, Punjab, India*

We present the power exchange dynamics between two closely kept metal-insulator-metal (MIM) structures that constitutes a surface plasmon polariton waveguide directional coupler. This composite MIM waveguide coupler is a miniature one. A comparative study of the power exchange and coupling dynamics is presented for Gold, Silver, Aluminium and Copper; the commonly used noble metals for MIM waveguides. Finite-difference-time domain method based full numerical experiments are performed to reveal the impact of the operating wavelength, refractive indices of the waveguides and other system parameters on the coupling profile of the plasmonic directional coupler. Unlike a conventional dielectric coupler MIM waveguide coupler shows linear increment in coupling length with increasing wavelength. Insertion of dielectric media in between the metal strips strengthens the coupling. The influence of nature of the metal-dielectric interfaces and waveguide asymmetry on the power coupling profile is demonstrated.

(Received October 5, 2020; accepted February 11, 2022)

Keywords: Plasmonic coupler, Directional coupler, Surface plasmon polariton, FDTD method

1. Introduction

The miniaturization of the photonics devices up to nanoscale has been challenged by the diffraction limit. The diffraction limit can be easily overcome by the use of surface plasmon polaritons (SPPs) [1, 2]. The SPPs are the evanescent waves traveling along with the interface between the positive refractive index (dielectrics) and the negative refractive index (noble metals) materials in the visible range of electromagnetic (EM) radiations. The quantization of the plasma oscillations of the free electron gas density of metal generates the quasi-particle named *plasmon*. When the plasmon interacts with the optical photon, it produces a coupled state called *plasmon polariton*. When surface plasmon, which is generated in the interface of the metal and the dielectric couples with the photon it leads to the formation of a coupled or hybrid state referred as SPPs. These SPPs propagate along the surface of metal until their energy is lost away by radiative leakage or absorption in the metal. The existence of surface plasmon was first demonstrated by Rufus Ritchie in 1957 [3]. As trapping and guiding of the electron is called electronics, similarly the trapping and guiding of the SPPs at nanoscale structures is commonly termed as *plasmonics* [4]. In recent decades, researchers have proposed a large range of applications in the field of plasmonics covering the biological nanosensors [5], nano-size imaging devices [6], fusion of electronic circuits with photonic components [7], etc. In particular, SPPs found extensive application in nano-size optical passive waveguide devices, such as filters [8], bends directional couplers [9-16], splitters [17], and Mach-Zehnder interferometers [18].

The multilayer-insulator waveguides are useful photonic structures as they are used in producing couplers, beam splitters, and modulators in integrated optics. The exchange of energy between the neighbouring waveguides is based on *coupled mode theory* [19]. Although, the theory as well as experiments on the multilayer-insulator waveguides are abundant in current literature some fine tuning is still missing. Thus, in the present communication, we study the power exchange dynamics in a MIMIM (*metal-insulator-metal-insulator-metal*) based plasmonic coupler for a dimension much smaller than the usual one. Such an arrangement has important features related to surface plasmon polariton guiding, interference and can be valuable for numerous experiments in plasmon optics. This may help in further miniaturization of the currently available MIMIM based devices as well as in understanding the sensitivity of power exchange on system parameters. Moreover, a comparative study with four frequently used metal is done to identify the more useful ones to optimize the coupler structure.

2. Coupler design and simulation

In plasmonics, the geometry of the elements under consideration is crucial for many important details: losses, field localization, scattering, etc. For example, in case of grooves, slits or DLSPPW as a parallel waveguide, the coupling efficiencies will be very different, since they depend strongly on field localization in a specific type of a waveguide. Besides, there are many other parameters that will depend strongly on the geometry chosen. For the current investigation we consider a five layers MIMIM (metal-insulator-metal-insulator-metal) plasmonic structure that constitutes a two-waveguide (MIM) coupler. Since, its working principle is based on SPP, henceforth we will refer this composite waveguide structure as MIM SPP waveguides. Besides, there are two other types of SPP waveguides, namely, dielectric loaded surface plasmon polariton waveguide (DLSPPW) and IMI (Insulator-Metal-Insulator) waveguides. Although, the DLSPPW and IMI have larger with respect to that in MIM waveguide, however, in spite of lower propagation length than DLSPPW and IMI waveguide the MIM waveguide is more preferred for miniaturization owing to its capability in light confinement in deep sub wavelength scale [20]. The dynamics of the EM wave and hence exchange of energy in coupled waveguides can be represented by the coupled-mode equations [19],

$$\frac{\partial \psi_1}{\partial z} = -j\delta\psi_1 - j\kappa\psi_2, \tag{1}$$

and

$$\frac{\partial \psi_2}{\partial z} = -j\delta\psi_2 - j\kappa\psi_1 \tag{2}$$

where ψ_1 and ψ_2 are the field amplitude of waveguide-1 and 2 respectively. κ is the coupling coefficient and δ is the phase mismatch factor. Full numerical simulation using the finite difference time domain (FDTD) method under perfectly matched boundary conditions [21] describe the energy exchange dynamics between the two waveguides.

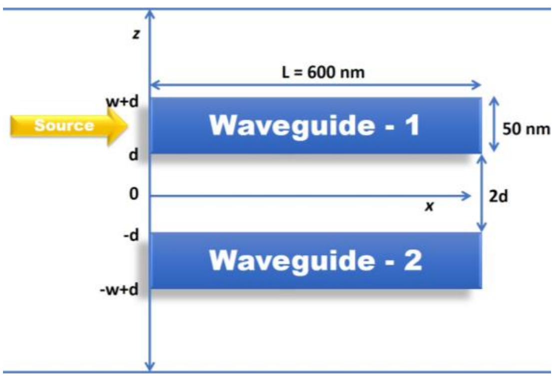

Fig. 1. Schematic diagram of MIMIM plasmonic coupler (color online)

In real experiments these waveguides are fabricated by cutting out two parallel grooves in a noble metal sheet. The noble metals are Silver (Ag), Gold (Au), Copper (Cu) or Aluminum (Al). These grooves, which could be filled with air or a linear transparent dielectric (insulator) materials can confine the electromagnetic (EM) energy. The schematic diagram of the structure under consideration is shown in Fig. 1. The EM radiation dynamics of the plasmonic waveguide coupler is explored by FDTD method, where we choose the system parameters as follows. The length 'L' of each of the waveguide is fixed as 600 nm, and the width 'w' of each waveguide is initially set to 50 nm. These waveguides are separated by a distance of 9 nm from each other. The mesh size is chosen as 2 nm for the FDTD simulation and the simulation is executed for 1000 time steps. The relative permittivity of the metal is calculated by Drude's model as [1],

$$\varepsilon_r = 1 - \frac{\omega_p^2}{\omega^2 + i\gamma\omega} \tag{3}$$

where ω_p is called the plasma frequency and γ is the damping constant. For our simulation, we have used the Johnson and Christy database [22]. The refractive index of air is 1 whereas refractive index of glass could vary from 1 to 1.6. Generally, we choose silver as a noble metal and the waveguide is filled with air unless specified. In all the figures showing power exchange profile, the dotted (Red) line represents the power in the waveguide-1 in which the EM radiation is launched (unless mentioned), whereas the solid (Blue) line represents the power in waveguide-2.

One of the main objectives of this theoretical investigation is to design an experimental model of MIM based plasmonic directional coupler. Any experimental realization requires flexibility of the model, more precisely, availability of a significant range of system parameters and materials. In view of this, in the forthcoming subsections A-E we discuss the effect of wavelengths, refractive indices, nature of metal-air interface and waveguide asymmetry on the coupling and show the coupler performance for a wide range of system parameters that will eventually ease the experimental designing.

A. Effect of the wavelength of radiation on the coupling length

In order to explore the effect of wavelength on the power coupling between the two plasmonic waveguides EM radiations of wavelengths ranging from 600 nm to 1600 nm are launched at waveguide-1. Power launched at the input end of the waveguide-1 is normalized to unity, while initially waveguide-2 does not have any power. As the radiation travels in the waveguide, the power of waveguide-1 starts shifting towards the waveguide-2 (Fig. 2). After a certain length along the waveguide coupler the powers in both waveguides become the same. This length of half-power transfer is called *half-power length* 'L_h'. Thereafter, the power of waveguide-1 reduces to zero while the power in waveguide-2 becomes maximum. This length, where the power transfer is complete (for symmetric waveguides) or maximum is referred as *coupling length* 'L_c'. Generally, $L_h = L_c/2$. The process of power exchange between waveguides continues until the power of the radiation does not fade away due to attenuation. Aforesaid power exchange dynamics is very common to a waveguide directional coupler. The coupling length does not depend on the total length of the coupler, rather depends on the overlapping of modal-field of the waveguides and hence propagation characteristics of the mode-fields through the individual waveguides as well as their separation. Besides these obvious dependences the coupling length significantly depends on the input wavelength. At larger wavelength of the input EM radiation the half-power length and hence the coupling length becomes longer (Fig. 2), i.e., *the exchange of energy between the waveguides is faster for the radiation of shorter wavelength*. This trend is completely opposite to that of a conventional dielectric waveguide as well as *DLSSPW*. An intuitive explanation of the same is provided in Ref. [20, 23]. According to those the coupling by overlapping of the evanescent fields occurs in the metallic region. The coupling coefficient 'κ' for the MIM SSP waveguide directional coupler can be given by,

$$\kappa \propto \exp\left(-\frac{2\pi\sqrt{n_{eff}^2 - \varepsilon_m}}{\lambda} d \right), \qquad (4)$$

where n_{eff} is the effective mode refractive index, ε_m is the permittivity of the metal, d is the gap between the waveguides and λ is the wavelength. In a conventional dielectric waveguide or DLSPPW the permittivity of the dielectric is positive and varies at much slower rate with the variation of λ. Thus the value of κ is mainly tuned by λ, which is inversely related to the former. Therefore, coupling length monotonically decreases and exchange of energy becomes faster with the increase of the wavelength. In contrary, for the present case, where the coupling is occurring in the metallic region, the ε_m of the metals significantly decreases with the increase in wavelength (although in different fashion for different metals) in such a way that the rate of increment of the numerator in the exponential term of equation (4) is greater than that of the denominator. Thus increase in wavelength witnesses an almost linear elongation of the coupling length in MIM SPP waveguide directional coupler.

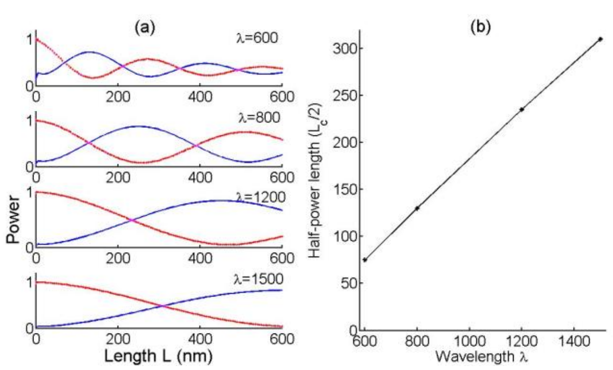

Fig. 2. (a) Power exchange between the waveguides of the plasmonic coupler along the waveguide length L at different wavelength for silver-air interface. (b) Variation of half-power Length $L_c/2$ with wavelength (color online)

B. Effect of metal-air interface on the coupling

In order to explore the impact of nature of the metal-air interface on the coupler dynamics we chose four different noble metals, namely, Silver, Gold, Copper and Aluminium to form the various interfaces with air. Figs (3) to (6) show the effect of this metal-air interface on the power coupling for different operational wavelengths. At a wavelength λ =1500 nm the coupling length is more or less the same for the Ag, Cu, and slightly shorter for Au but significantly longer for Al. For a lower operational wavelength, as expected, the half-power length decreases and hence coupling becomes faster for all the metal-air interfaces. However, at a wavelength as lower as 600 nm the coupling is weak for the Cu, while the performance of Ag and Au are very much ideal. A comparative wavelength dependence profile of the half-power length for different metals is portrayed in Fig. 7. The performance of Al is a bit more reliable with respect to Cu but its longer coupling length and hence slower coupling send it to the back foot unless the cost of the metal is a constraint.

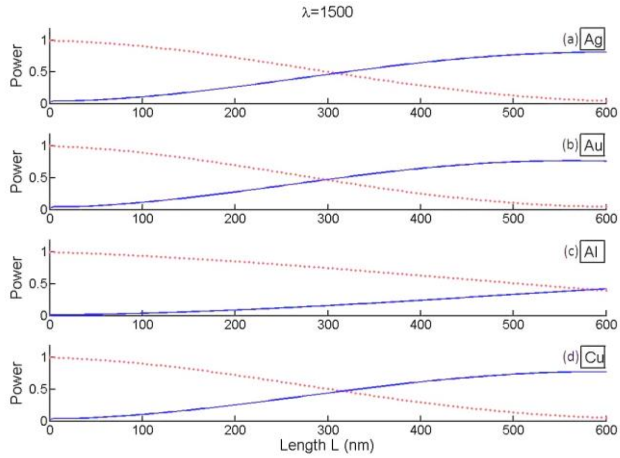

Fig. 3. Power exchange between the waveguides of the plasmonic coupler along the waveguide length for different metal-air interface at wavelength λ=1500 nm (color online)

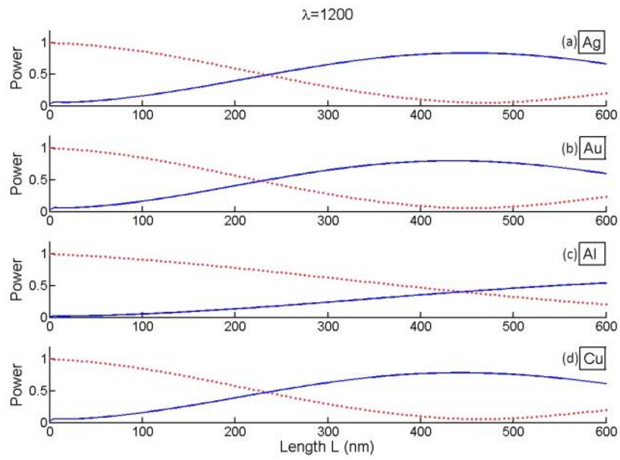

Fig. 4. Same as Fig. 3 at a wavelength λ=1200 nm (color online)

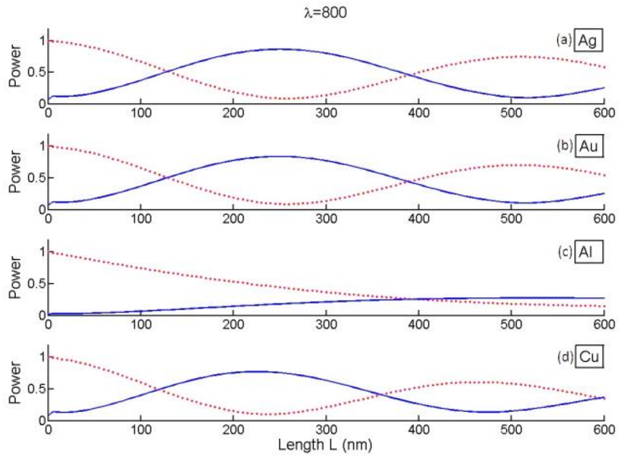

Fig. 5. Same as Fig. 3 at a wavelength $\lambda = 800$ nm (color online)

C. Effect of refractive index of waveguide materials on power coupling

In preceding subsections, a metal-air interface for the coupler is used. We now replace the air with glasses (that forms metal-glass interface) of different refractive indices, i.e., 1.45, 1.50 and 1.55 to capture the effect of refractive index on the coupling length and overall coupling dynamics. For a glass with higher refractive index coupling length becomes shorter (Fig. 8). Here, we present the case for Ag-glass interface or Ag-glass-Ag-glass-Ag coupler structure. Similar effect of the refractive index is observed for other metal-glass interfaces, with an already mentioned poor coupling for Cu at lower wavelengths.

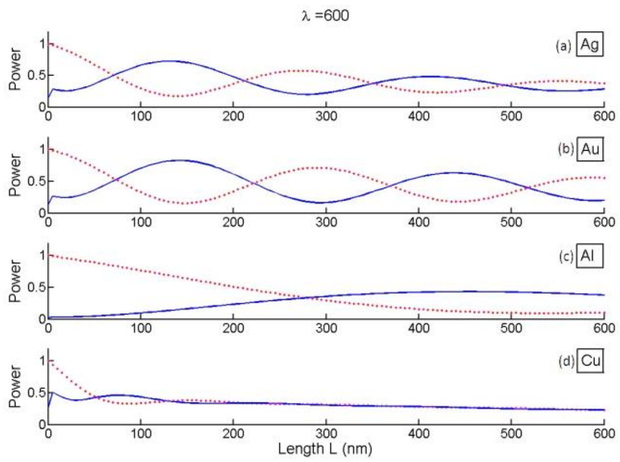

Fig. 6. Same as Fig. 3 at a wavelength $\lambda = 600$ nm (color online)

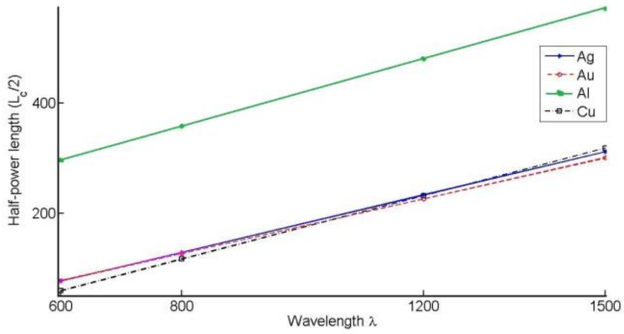

Fig. 7. Variation of half-power length $L_c/2$ with wavelength for Ag, Au, Al and Cu (color online)

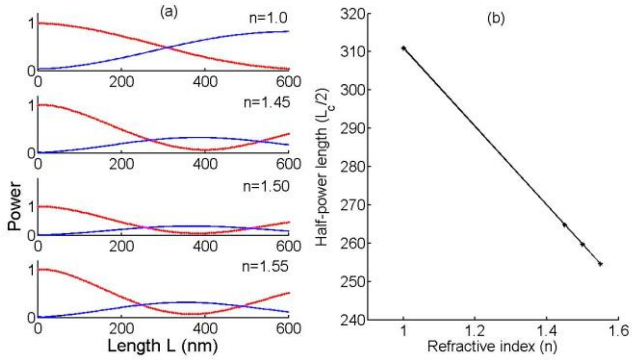

Fig. 8. (a) Variation of power in the Ag-glass-Ag-glass-Ag coupler along the waveguide length 'L' for glasses of different refractive indices 'n' at $\lambda = 1500$ nm. (b) Variation of half-power length (or $L_c/2$) with refractive index (color online)

D. Effect of asymmetry in the thickness of waveguide on the coupling length

All the plasmonic couplers we considered till now have two similar waveguides, i.e., of the same thickness and same metal-dielectric interfaces. The power exchange dynamics significantly changes for asymmetric waveguides. To demonstrate this, we simulate two sets of coupler structure, the first one having thickness of the waveguide-1 and 2 equal to 60 nm and 50 nm, respectively and in the second one the thicknesses are interchanged. That means both are asymmetric waveguide-couplers and the thickness of the power launching waveguide is different. Remaining parameters are the same as in Fig. 2. The first set (Asymmetric-1) results in Fig. 9 while the second set (Asymmetric-2) yields a coupling dynamics as in Fig. 10. A simple observation cannot reveal any significant difference in coupling profiles between the two at lower wavelength (Fig. 11). However, a comparison reveals that both the asymmetric structures have lower half-power length than the symmetric waveguide structure at any given wavelength. This gap becomes more prominent at higher wavelengths. Moreover, Asymmetric-2 structure has slightly lower coupling length in comparison to the Asymmetric-1. All these suggest that a minor asymmetry in the waveguides does not impact much the power coupling dynamics at smaller wavelength but exaggerate at higher wavelength.

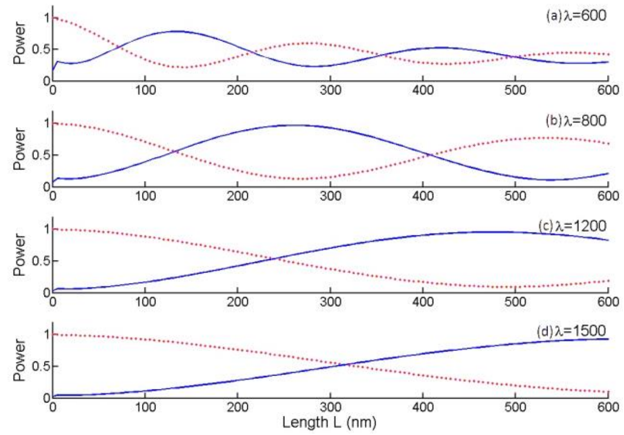

Fig. 9. Power coupling dynamics with waveguide-1 of thickness 60 nm and waveguide-2 of thickness 50 nm (color online)

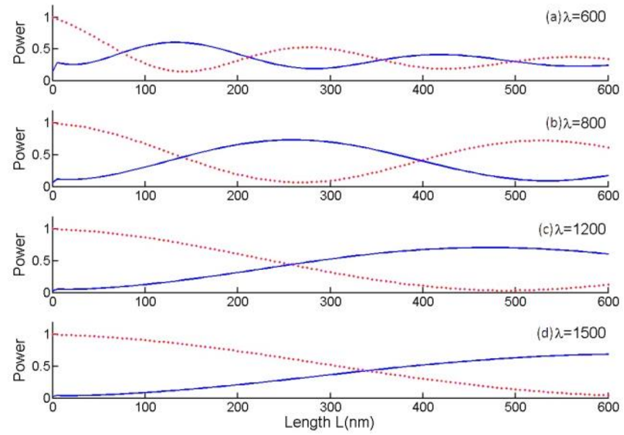

Fig. 10. Power coupling dynamics with waveguide-1 of thickness 50 nm and waveguide-2 of thickness 60 nm, i.e., the thickness of the power launching waveguide is now narrower. Rest of the parameters as in Fig. 9 (color online)

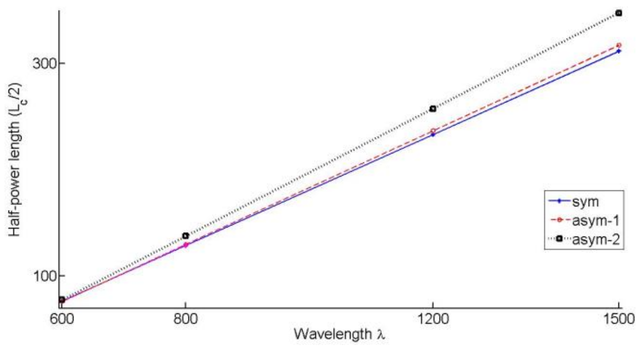

Fig. 11. Comparison of the dependence of half-power length $L_c/2$ *on wavelength for (a) symmetric (b) and (c) Asymmetric (color online)*

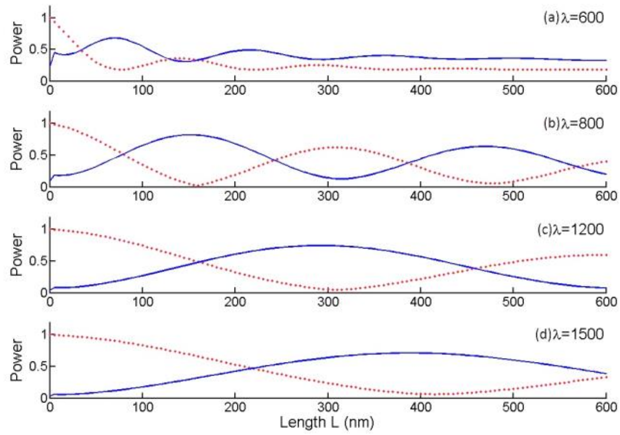

Fig. 12. Coupling dynamics in Ag-glass-Ag-air-Ag plasmonic coupler. Waveguide-1 is of glass n=1.5 and waveguide-1 is air-filled n=1 (color online)

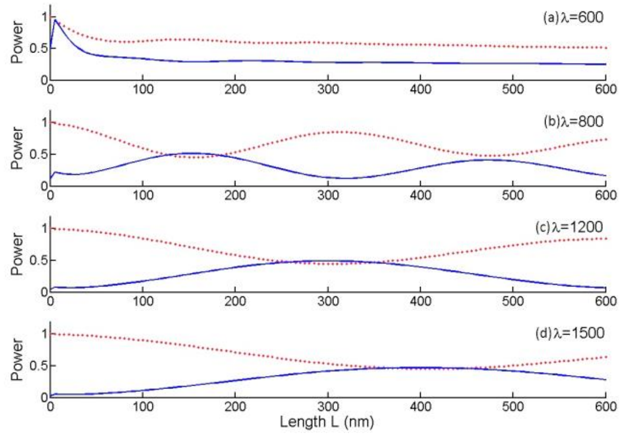

Fig. 13. Coupling dynamics in Ag-air-Ag-glass-Ag plasmonic coupler. Waveguide-1 is now filled with air, while the other is with glass n=1.5 a. Rest of the parameters are as in Fig. 12 (color online)

E. Effect of asymmetry in refractive indices of the waveguide on coupling length

Like the asymmetry in thickness the asymmetry in refractive indices of the waveguide materials may influence the coupling dynamics. To reveal the same, we take a plasmonic coupler, wherein one waveguide is air filled (i.e., n=1.0) and the other is glass (n=1.5) waveguide. First we launch the power at glass waveguide and in the second case at the air waveguide. The corresponding power exchange profiles (Fig. 12 for the first case and in Fig. 13 for the second case) portray that the coupling performance deteriorate at lower operating wavelength. It almost ceases at 600 nm particularly for second case. Also the power transfer from glass to air waveguide is faster and more efficient as compared to power transfer from air to glass waveguide.

In the present investigation we consider low to moderate amplitude of the input signal, which ensures either zero or negligible nonlinear effects. Although, when a high amplitude signal is used the nonlinear effects get exaggerated, yet the basic coupler performance is governed by the linear response. However, nonlinear effects may lead to some complex phenomena that can be beneficially used to enhance the coupler performance, e.g., to construct a solitonic coupler.

3. Conclusion

We portray the influence of the operating wavelength, nature of the interface, asymmetry in plasmonic waveguides on the power coupling and power exchange profiles of a miniature MIMIM Plasmonic (or MIM SPP) waveguide coupler. The coupling length linearly increases with the operating wavelength, i.e., that of the input EM radiation. While Gold and Silver are more suitable metal for making such plasmonic coupler, Aluminium can be a cheaper substitute. However, Copper is a bad option particularly at lower wavelengths. The asymmetry in waveguide thickness may be noticeable at higher wavelength. Interestingly, the power transfer from glass waveguide to air-filled waveguide in such plasmonic coupler is faster than from air-filled wave guide to glass one. Therefore, increasing the refractive index of the waveguide slab the coupling length can be reduced, which is a useful point for further miniaturization of the coupler. The methodology of investigation can be extended to many other designs of MIMIM plasmonic (or MIM SPP) waveguide couplers. The results of this investigation can be used to construct a MIMIM plasmonic waveguide based power splitter, sensor, polarization splitter. Also these results may guide for further miniaturization of existing MIMIM plasmonic couplers.

Acknowledgments

The author MM is thankful to DST-SERB for the research grant via fast track project no FTP/PS-211/2012. Soumendu Jana would like to acknowledge the financial supports of Ministry of Electronics & Information Technology, MeitY, Govt. of India, through “Young Faculty Research Fellowship under Visvesvaraya PhD Scheme” (Ref: MLA / MUM /GA / 10(37) B) and Science & Engineering Research Board (SERB), Govt. of India, through core research grant (File Number: CRG/2019/005073).

References

[1] S. A. Maier, Plasmonics: Fundamentals and Applications, Springer, 2007.
[2] E. N. Economu, Phys. Rev. **182**, 539 (1969).
[3] R. H. Ritchie, Physical Review **106**, 874 (1957).
[4] A. Polman, H. A. Atwater, Materials Today **8**, 56 (2005).
[5] J. N. Anker, W. P. Hall, O. Lyanders, N. C. Shan, J. Zhao, R. P. Van Duyne, Nature Mater. **7**, 442 (2008).
[6] N. Fang, H. Lee, C. Sun, X. Zhang, Science **308**, 534 (2005).
[7] E. Ozbay, Science **311**, 189 (2006).
[8] J. Tao, X. G. Huang, X. S. Lin, Q. Zhang, X. P. Jin, Opt. Express **17**, 13989 (2009).
[9] H. Zhao, X. Guang, J. Huang, Physica E **40**, 3025 (2008).
[10] D. Chelladurai, M. Doderer, U. Koch, Y. Fedoryshyn, C. Haffner, J. Leuthold, Opt. Express **27**, 11862 (2019).
[11] M. Olyaee, M. Tavakoli, A. Mokhtari, Opt. Quant. Electron **50**, 404 (2018).
[12] F. Ding, S. I. Bozhevolnyi, IEEE Journal of Selected Topics in Quantum Electronics **25**, 1 (2019).
[13] C. E. Garcia-Ortiz, V. Coello, E. Pisano, Y. Chen, S. I. Bozhevolnyi, Opt. Express **27**, 22753 (2019).
[14] S.Tan, A. Argondizzo, J. Ren, L. Liu, J. Zhao, H. Petek, Nature Photon. **11**, 806 (2017).
[15] A. Dolatabady, N. Granpayeh, Plasmonics **12**, 597 (2017).
[16] S. Jana, S. Konar, M. Mishra, Zeitschrift fur Naturforschung - Section A, Journal of Physical Sciences **63**, 145 (2008).
[17] G. Veronis, S. Fan, Appl. Phys. Lett. **87**, 131102 (2005).
[18] S. Bozhevolnyi, V. Volkov, E. Devaus, J. Laluet, T. W. Ebbesen, Nature **440**, 508 (2006).
[19] Wei-Ping Huang, J. Opt. Soc. Am. A **11**, 963 (1994).
[20] Mingbo Pu, Na Yao, Chenggang Hu, Xuecheng Xin, Zeyu Zhao, Changtao Wang, Xiangang Luo, Opt. Express **18**, 21030 (2010).
[21] Umran S. Inan, Robert A. Marshall, Numerical electromagnetics : the FDTD method, Cambridge University Press, New York (2011).
[22] P. B. Johnson, R. W. Christy, Phys. Rev. B **6**, 4370 (1972).
[23] C. L. Chen, Foundations for Guided-Wave Optics, Wiley (2006).

*Corresponding author: soumendu.jana@thapar.edu